Conf-890933--3
BNL-42492

BNL--42492

DE90 000531

NUCLEAR BRAGG X-RAY SCATTERING OF SYNCHROTRON RADIATION BY $^{57}Fe_2O_3$: METHODOLOGY AND STUDIES OF DYNAMICAL PROCESSES*

P.E. Haustein, L.E. Berman, G. Faigel*, J.R. Grover,
J.B. Hastings and D.P. Siddons,
Brookhaven National Laboratory, Upton, N.Y. 11973, USA

ABSTRACT

A program of studies of nuclear Bragg X-ray scattering with $^{57}Fe_2O_3$ at the National Synchrotron Light Source at Brookhaven National Laboratory and at the Cornell University CHESS facility is reviewed. Two main areas, instrumentation development and studies of dynamical diffraction processes, are described. The latter area has included: measurements of the temporal behaviour of nuclear collective decay mode and direct observation of polarization mixing.

INTRODUCTION

Nuclear Bragg scattering (NBS) of synchrotron radiation (SR) has been shown to yield filtered X-ray beams with extremely narrow bandwidth (10^{-6}-10^{-8}eV), small angular divergences, and unique polarization and temporal properties. These characteristics, unobtainable with radioactive sources, result from the coupling of the properties of synchrotron radiation to those of the nuclear resonance process. They are expected to open up new areas of research with important diverse applications in chemistry, physics and material sciences.

DISCUSSION

Early efforts at BNL concentrated on the development of instrumentation specifically optimized for NBS studies. It is clear that suppression, by large factors, of the off-resonance photons from the SR continuum can significantly simplify the experimental detection of nuclear resonance processes. A six reflection premonochromator [1,2] employing two stage reflection from Si (1,1,1), followed by four stages of reflections from Si (10,6,4) is shown in Fig. 1. At the 14.4 keV ^{57}Fe Mössbauer resonance it provides extremely high energy resolution (5 meV) and small angular width (0.4 arcsec). Thus crystalline Mössbauer materials may be excited at the nuclear Bragg angle with excellent suppression of incoherent scattering. Using this device and a highly perfect Fe_2O_3 single crystal, isotopically enriched with ^{57}Fe to 93 %, rocking curves and energy scans, Fig. 2., for the electronic (6,6,6) and pure nuclear (7,7,7) reflections were obtained. The 250 meV width of the (6,6,6) reflection is consistent with the 3 arcsec rocking curve which is dominated by the small crystal imperfection. The energy width of the (7,7,7) reflection, however, is just 5 meV and mirrors the intrinsic resolution of the premonochromator. These measurements confirm the pure nuclear origin of the (7,7,7) reflection; neither magnetic of multiple X-ray scattering are plausible alternatives since they would also be dominated by the crystal deformations and, concomitantly, have energy spreads like that of the (6,6,6) reflection.

Coupling of the unique timing properties of SR with temporal aspects associated with coherent excitation of ordered arrays of nuclear scatterers is an extremely convenient way to measure dynamical processes in NBS and to confirm predictions of the theory [4,5]. One important feature is the large reduction in the effective nuclear decay lifetime which can be explained by the coherent nature of the excited states in perfect crystals, and another is the modulation of the decay rate that arises from the interference among the ^{57}Fe hyperfine levels. Timing studies of this type were performed by (1) augmenting the apparatus of Fig. 1. with a P-I-N diode in the SR beam that provided a t=O reference signal, by (2) applying a static external magnetic field of ≈ 1 kG to the crystal and by (3) using a BaF_2 detector and fast phototube in place of the Ge detector. Time spectra for the (7,7,7) reflection were accumulated. Fig. 3. shows a smoothed experimental spectrum which has had the prompt backround removed. The continuous curve is the result of a dynamical diffraction calculation [6]. Note that the complete time evolution is followed from the instant of the excitation.

Another interesting area of NBS to explore is that of polarization mixing with SR. In the case of $^{57}Fe_2O_3$ the non--degeneracy of the $\Delta m = 0,\pm 1$ hyperfine levels gives rise to linear or circularly polarized oscillators. Theory predicst that the polarization of the incident SR beam may be modified upon Bragg reflection. To confirm such predictions the apparatus shown in Fig. 4. was added [7]. Key elements are the use of a nearly perfect Be single crystal as a polarization analyzer and a rotatable Sm-Co permanent magnet that affects the small ferromagnetic moment of the α-hematite and allows alignment of the quantization axis with respect to the scattering plane. The polarization analyzer could be set to transmit either σ- or π-polarized radiation; data were taken with changes of the magnetic quantization axis from 0° to 90° in 15° steps. Representative rocking curves for α-$^{57}Fe_2O_3$ (7,7,7) reflections are shown in Fig. 5.(a) (σ polarization transmitted) and 5.(b) (π polarization transmitted). Open points in Fig. 5.(a) correspond to the weak π-component in the SR beam being switched to σ-polarization. In Fig. 5.(b) the closed points represent the nonmixing π-π scattering, but from theory it is known that the π polarization does not couple to any transition in this case yielding a lower "background" than in the preceding case. The closed points in Fig. 5.(a) and the open points in Fig. 5.(b) represent the σ-σ and σ-π scattering respectively and clearly show a strong dependence of the polarization of scattered photons on the external magnetic field direction. The observed effects are in accord with theory and they demonstrate that it is possible to filter SR X-ray beams so that very long coherence lengths with switchable polarization orientations can be achieved in the filtered beam.

CONCLUSION

In summary, nuclear resonant Bragg scattering has been shown to be an effective method for filtering SR beams. Many unique properties of the incident beam (such as time resolution) are retained while the filtered beams possess extraordinarily high energy resolution, small angular divergence, and conveniently adjustable polarization properties. General applicability of NBS filtering will be possible at a variety of X-ray wavelengths as other isotopic systems are exploited.

* Research performed under the auspices of the U.S. Department of Energy under Contract DE-AC02-76CH00016.

+ Permanent address: Central Research Institute for Physics, Budapest, Hungary.

Running headline: HAUSTEIN NUCLEAR BRAGG SCATTERING

REFERENCES

1. G. Faigel, D.P. Siddons, J.B. Hastings, P.E. Hausten, J.R. Grover, J.P. Remeika, A.S. Cooper, Phys. Rev. Lett. 58, (1987), 2699.
2. D.P. Siddons, J.B. Hastings, G. Faigel, L.E. Berman, P.E. Haustein, J.R. Grover, Rev. Sci. Instrum. in press.
3. G.T. Trammell, in Chemical Effects of Nuclear Transactions (IAEA Vienna, 1961), vol. 1, p. 75.
4. J.P. Hannon and G.T. Trammell, Phys. Rev. 186, (1969), 306.
5. Yu. Kagan, A.M. Aganas'ev, and V.G. Khon, J. Phys. C12, (1979), 615.
6. G. Faigel, D.P. Siddons, J.B. Hastings, P.E. Haustein, J.R. Grover, L.E. Berman, Phys. Rev. Lett. 61, (1988), 2794.
7. D.P. Siddons, J.B. Hastings, G. Faigel, L.E. Berman, P.E. Haustein, J.R. Grover, Phys. Rev. Lett. 62, (1989), 1384.

FIGURE CAPTION

Fig. 1. Schematic view of the experimental arrangement.

Fig. 2. Rocking curves (a) and energy scans (b) of the (6,6,6) and (7,7,7) reflections. The continuous lines are guides for the eye.

Fig. 3. Time evolution of the "pure-nuclear" (7,7,7) reflection of α-hematite. The continuous curve corresponds to a dynamical diffraction calculation, see ref. 6.

Fig. 4. A schematic view of the diffractometer which carries the sample, its polarizing magnet and the polarization analyzer crystal.

Fig. 5. (a) rocking curve at resonance for orientations of the magnetic quantization axis parallel and perpendicular to the scattering plane, with the polarization analyzer set to transmit σ-polarized radiation. (b) as (a), but for the case with the polarization analyzer set to transmit π-polarized radiation. Unit vectors $\hat{u}_z$ refer to the quantization axis vectors.

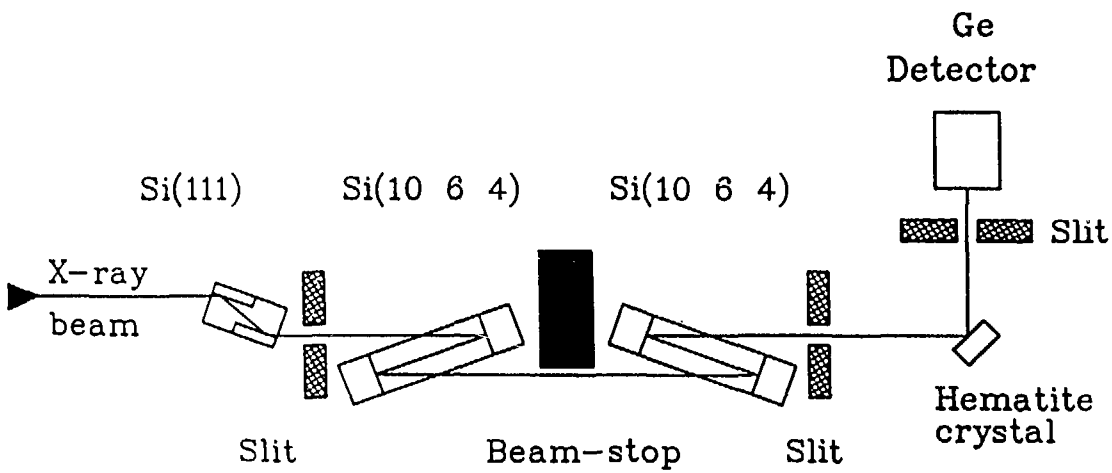

Ge
Detector
Si(111)
Si(10 6 4)
Si(10 6 4)
Slit
X-ray
beam
Slit
Beam-stop
Slit
Hematite
crystal

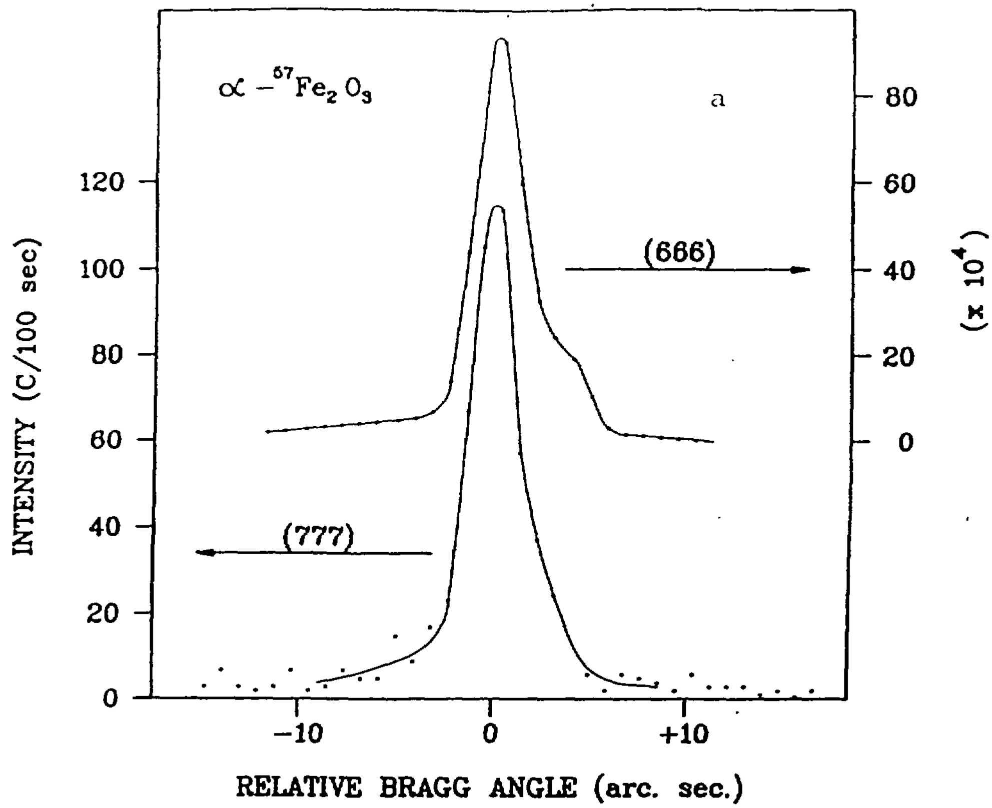

α – $^{57}Fe_2O_3$
a
(666)
(777)
INTENSITY (C/100 sec)
(x 10^4)
RELATIVE BRAGG ANGLE (arc. sec.)

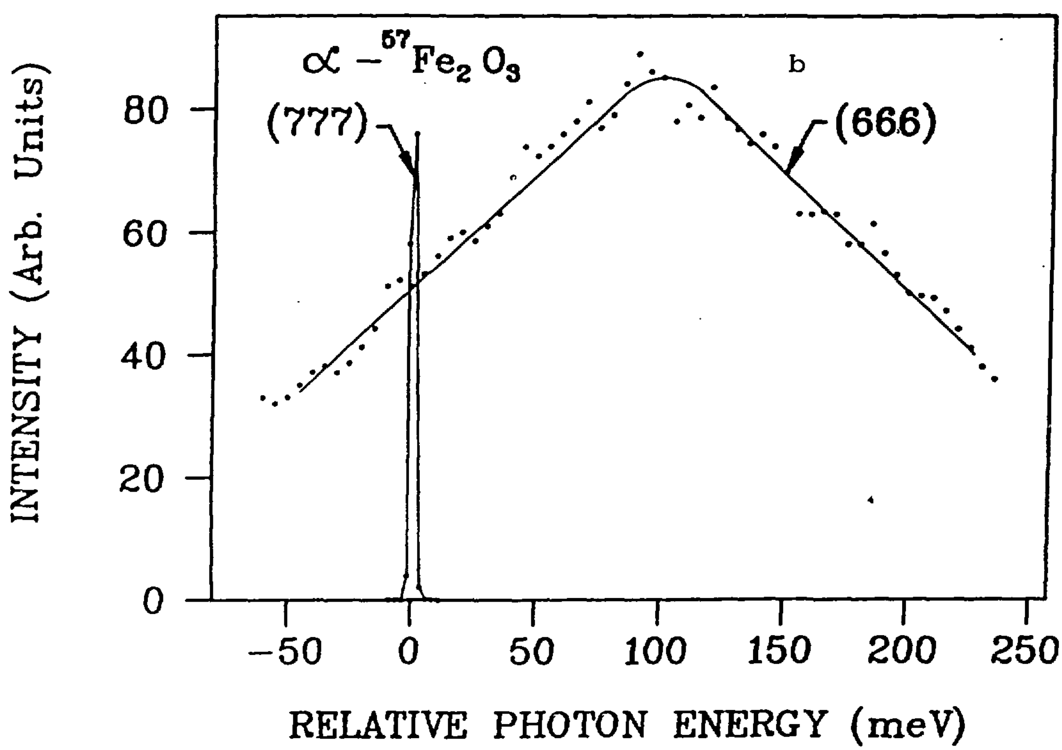

α – $^{57}Fe_2O_3$
b
(777)
(666)
INTENSITY (Arb. Units)
RELATIVE PHOTON ENERGY (meV)

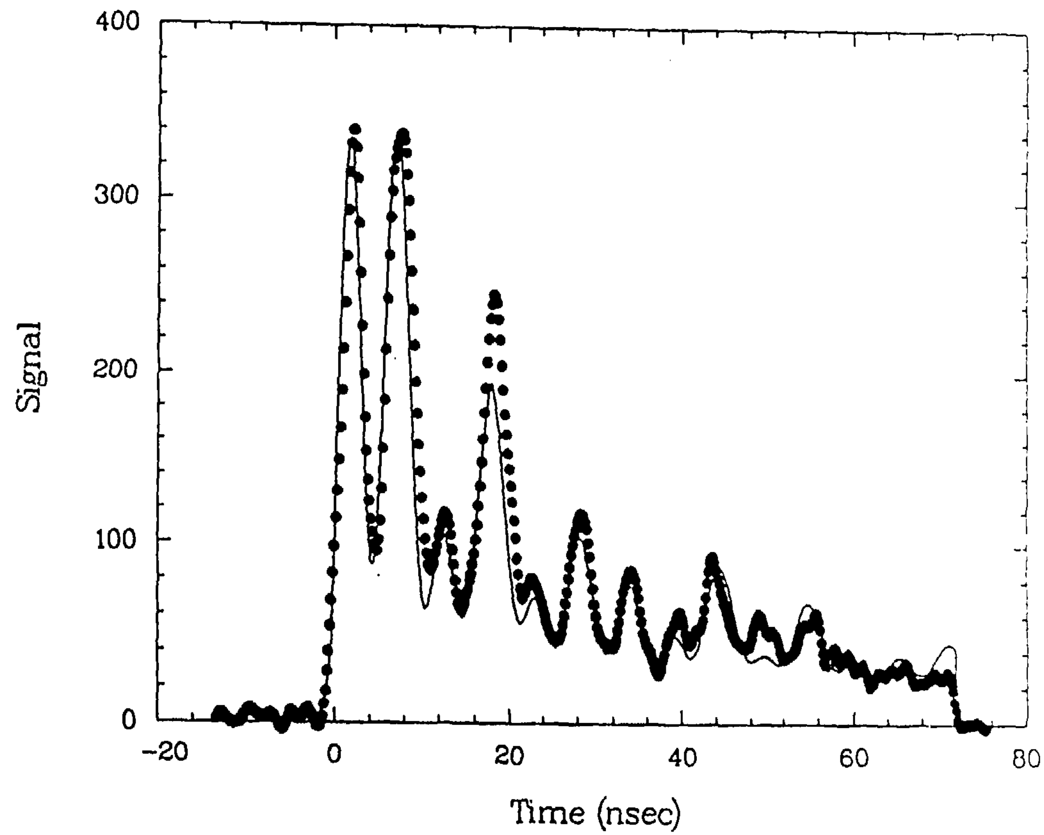
Signal
400
300
200
100
0
-20
0
20
40
60
80
Time (nsec)

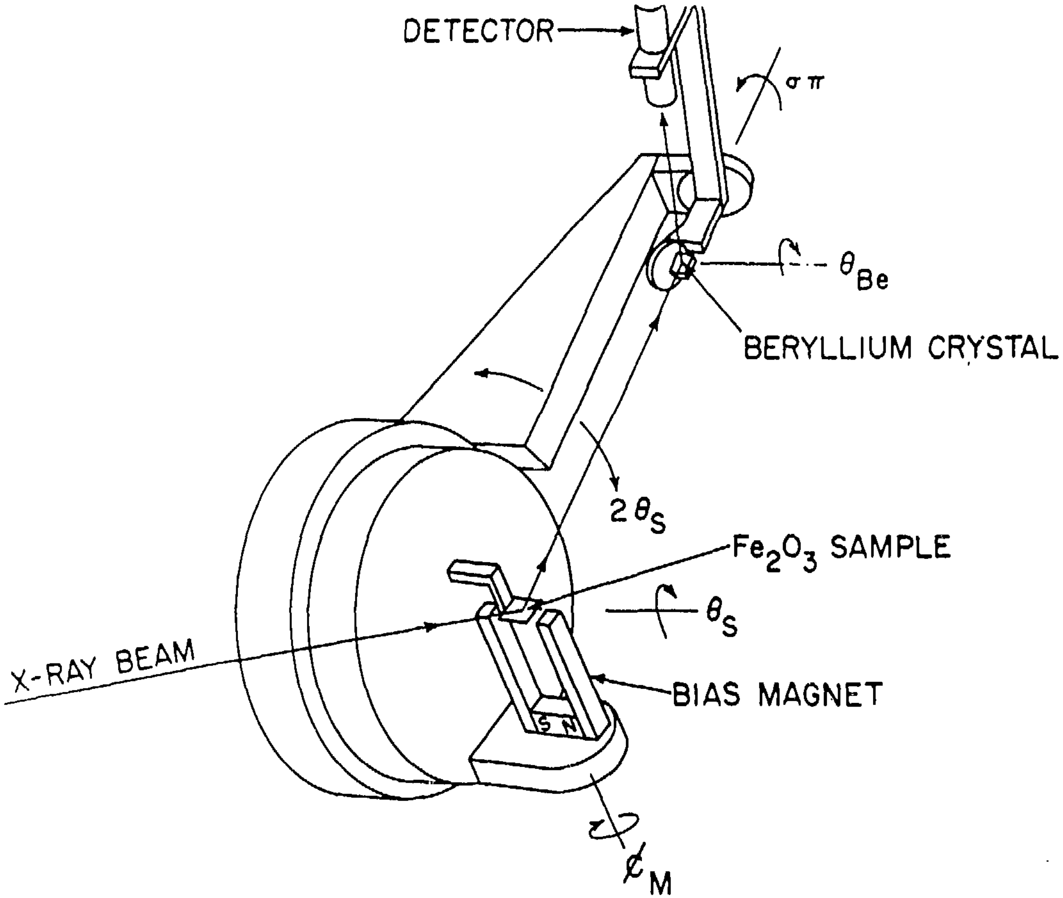
DETECTOR
σ π
θBe
BERYLLIUM CRYSTAL
2θS
Fe2O3 SAMPLE
θS
X-RAY BEAM
BIAS MAGNET
S N
ϕM

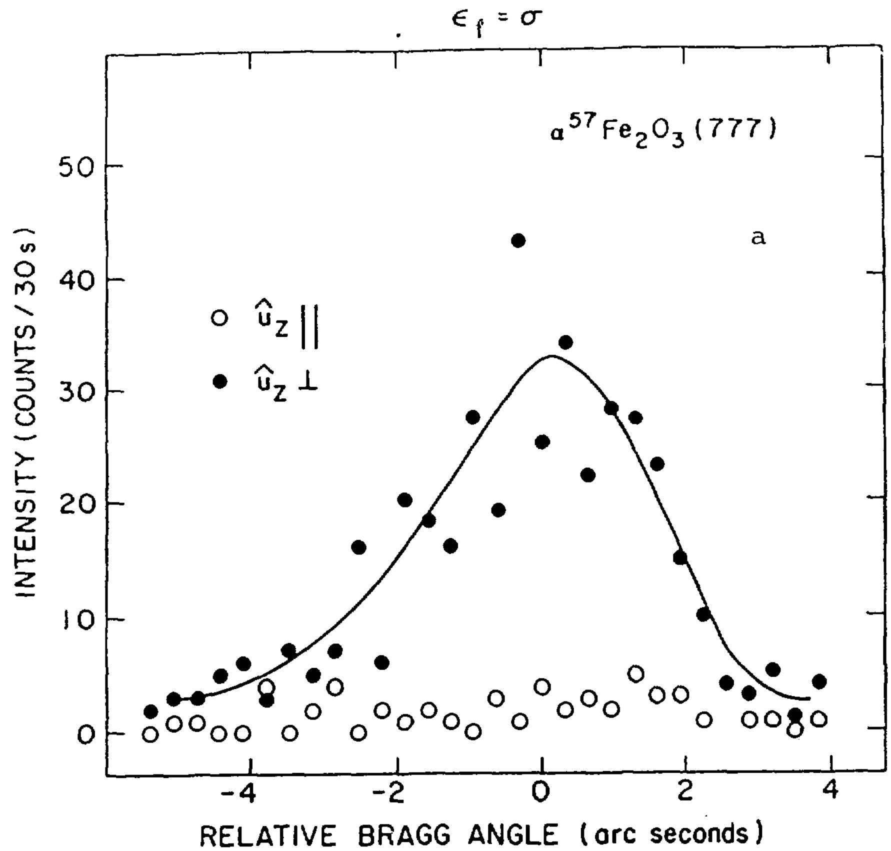
$\epsilon_f = \sigma$
$\alpha\,^{57}Fe_2O_3$ (777)
a
$\hat{u}_z \parallel$
$\hat{u}_z \perp$
INTENSITY (COUNTS / 30 s)
0
10
20
30
40
50
-4
-2
0
2
4
RELATIVE BRAGG ANGLE (arc seconds)

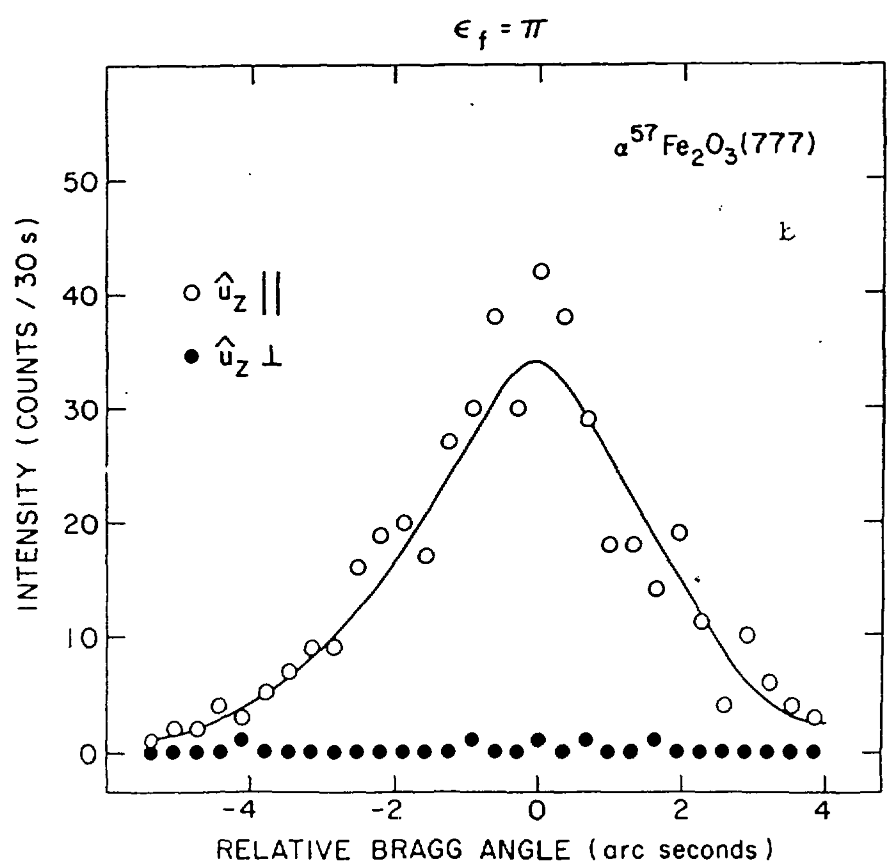
$\epsilon_f = \pi$
$\alpha\,^{57}Fe_2O_3$(777)
b
$\hat{u}_z \parallel$
$\hat{u}_z \perp$
INTENSITY (COUNTS / 30 s)
0
10
20
30
40
50
-4
-2
0
2
4
RELATIVE BRAGG ANGLE (arc seconds)